

LOWEST-DEGREE POLYNOMIAL DE RHAM COMPLEX ON GENERAL QUADRILATERAL GRIDS

QIMENGQUAN, XIA JI, SHUO ZHANG

ABSTRACT. This paper devotes to the construction of finite elements on grids that consist of general quadrilaterals not limited in parallelograms. Two finite elements are established for the H^1 and $H(\text{rot})$ elliptic problems, respectively. The two finite element spaces on general quadrilateral grids, together with the space of piecewise constant functions, formulate a discretised de Rham complex. First order convergence rate can be proved for both of them under the asymptotic-parallelogram assumption on the grids.

The local shape functions of the two spaces are piecewise polynomials, and the global finite element functions are nonconforming. A rigorous analysis is given in this paper that it is impossible to construct a practically useful finite element defined as Ciarlet's triple whose shape functions are always piecewise polynomials and which can form conforming subspaces on a grid that consists of arbitrary quadrilaterals.

1. INTRODUCTION

There has been a long history on the study of finite element methods on general quadrilateral grids. Many conforming and nonconforming finite elements are established for various model problems. The classical strategy for constructing quadrilateral elements is to utilize isoparametric technique (cf., e.g., [5]). With this strategy, one begins with a given shape function space on a reference square and a class of bilinear transforms (or Piola transforms, etc.), the finite element on any convex quadrilateral cell can be constructed correspondingly. Great success has been achieved via this approach, particularly in constructing conforming finite element spaces; we refer to [2, 3, 7] for more details. On the other hand, a solid difficulty of these methods, as discussed in, e.g., Zhang [14], is that one will encounter the problem of rational function integration in practical numerical computation due to non-constant Jacobian determinants and inverse Jacobian matrices. Besides, when we take the discretized differential complexes, which is one of the most fundamental structural feature of the finite element schemes and has been a central topic of the finite element methods during the passed decades, into consideration, we

1991 *Mathematics Subject Classification.* 65N35; 15A15.

Key words and phrases. nonconforming finite element; de Rham complex; general quadrilateral grids.

The research of X. Ji is supported by the National Natural Science Foundation of China under grants 91630313 and 11971468, and National Centre for Mathematics and Interdisciplinary Sciences, CAS. The research of S. Zhang is supported partially by the National Natural Science Foundation of China with Grant Nos. 11471026 and 11871465 and National Centre for Mathematics and Interdisciplinary Sciences, CAS.

have to pay extra attention to the different but relevant Jacobian matrices for the spaces, respectively. We are thus motivated to study finite element schemes with piecewise polynomials on every cell that possess clearer structure and more friendly implementation. In this paper, we present three finite element spaces on grids that consist of general quadrilaterals, and they form a discrete analogue of the de Rham complex which reads in 2D

$$(1) \quad \mathbb{R} \xrightarrow{\text{inclusion}} H^1 \xrightarrow{\nabla} H(\text{rot}) \xrightarrow{\text{rot}} L^2 \xrightarrow{\text{integration}} \mathbb{R}.$$

There have been various finite element schemes on general quadrilateral grids with piecewise polynomials; we refer to [8, 9, 11, 15] for example. Also, the first finite element complex with piecewise polynomials on general quadrilateral grids can be found in [15]. It is worthy of attention that all these aforementioned finite element spaces are nonconforming, except those for the space L^2 . Indeed, as will be proved in Section 2, it is impossible to construct a practically useful finite element whose shape functions are always piecewise polynomials and which can form conforming subspaces on a grid that consists of arbitrary quadrilaterals rather than parallelograms only. We thus do not seek to construct conforming elements; in view of (1), we impose the continuity of evaluation on vertices for the approximation of H^1 functions and the continuity of the average of the tangential component along the edges for the approximation of $H(\text{rot})$ functions, and these spaces can be called quasi-conforming ones. For low-degree polynomials, the continuity can guarantee the conformity of the respective finite element spaces on parallelograms, while on general quadrilaterals, the continuity does not even guarantee the functions to pass the patch test. In the analysis and the implementation, we will then adopt the general $O(h^2)$ asymptotic-parallelogram regularity assumption for the convergence. This assumption is normally used for the analysis of nonconforming finite element schemes. Further, due to the lack of full elliptic regularity, for the nonconforming finite element scheme of the $H(\text{curl})$ problem, higher than general regularity assumption may in general be needed for the same convergence rate. In contrast, by the aid of this assumption, we can prove the optimal convergence rate for the proposed elements with the proper regularity assumptions of the exact solutions. Though is crucial for our lowest-degree case, the assumption can be weakened for higher degree schemes, such as [1, 6].

The remaining of the paper is organized as follows. In the remaining of this section, we introduce some necessary notations. In Section 2, we introduce some geometrical features of the grids. We will particularly prove that, shortly speaking, no practically useful conforming element with piecewise polynomials can be constructed for general quadrilateral grids. In Section 3, three finite elements are introduced with a commutative diagram. The approximation error is analyzed by the technique of combining the classical Taylor expansion procedure and a specific commutative property. In Section 4, the modulus of the continuity of the finite element functions are given. Then in Section 5, the performance of the finite elements are studied for the

H^1 and $H(\text{rot})$ problems; both theoretical analysis and numerical verifications are given. Some conclusions and comments are given in Section 6.

Notations. In this paper, conventional notations for the Sobolev spaces and grid-related quantities will be used. Let $\Omega \subset \mathbb{R}^2$ be a simple connected Lipschitz domain and $\Gamma = \partial\Omega$ be the piecewise boundary with \underline{n} the outward unit normal vector and \underline{t} the counterclockwise unit tangential vector, “ $\underline{\cdot}$ ” representing the vector valued quantities. Denote by $H^m(\Omega)$ and $H_0^m(\Omega)$ the standard Sobolev spaces equipped with the norm $\|\cdot\|_{m,\Omega}$ and seminorm $|\cdot|_{m,\Omega}$ as usual, and $L_0^2(\Omega) := \{q \in L^2(\Omega) : \int_{\Omega} q \, dx = 0\}$. We also denote by $\underline{L}^2(\Omega) = (L^2(\Omega))^2$, $\underline{H}^m(\Omega) = (H^m(\Omega))^2$ and $\underline{H}_0^m(\Omega) = (H_0^m(\Omega))^2$. The inner product of L^2 and \underline{L}^2 is denoted by (\cdot, \cdot) on the domain Ω . We define two forms of rotation operator in two-dimensional case by

$$\begin{aligned} \text{Given a vector } \underline{\sigma}(x_1, x_2) = (\sigma_1, \sigma_2)^T & \quad \text{rot} \underline{\sigma} = \frac{\partial \sigma_2}{\partial x_1} - \frac{\partial \sigma_1}{\partial x_2} \\ \text{Given a scalar function } \sigma = \sigma(x_1, x_2) & \quad \text{curl} \underline{\sigma} = \left(\frac{\partial \sigma}{\partial x_2}, -\frac{\partial \sigma}{\partial x_1} \right)^T. \end{aligned}$$

Superscript T indicates transposition of vector or matrix as usual. We also use these notations to denote Sobolev spaces $H(\text{rot}, \Omega) = \{\underline{\sigma} | \underline{\sigma} \in \underline{L}^2(\Omega), \text{rot} \underline{\sigma} \in L^2(\Omega)\}$ and $H_0(\text{rot}, \Omega) = \{\underline{\sigma} | \underline{\sigma} \in H(\text{rot}, \Omega), \underline{\sigma} \cdot \underline{t} = 0 \text{ on } \Gamma\}$ equipped with standard norm $\|\cdot\|_{\text{rot},\Omega}^2 = \|\cdot\|_{0,\Omega}^2 + |\cdot|_{\text{rot},\Omega}^2$. Specially, a new notation is used for the space $H^1(\text{rot}, \Omega) \triangleq \{\underline{\sigma} | \underline{\sigma} \in \underline{H}^1(\Omega), \text{rot} \underline{\sigma} \in H^1(\Omega)\}$.

Let \mathcal{J}_h be a regular subdivision of domain Ω , with the elements being convex quadrilaterals, i.e., $\Omega = \cup_{K \in \mathcal{J}_h} K$. And any two distinct quadrilaterals K_1 and K_2 in \mathcal{J}_h with $\bar{K}_1 \cap \bar{K}_2 \neq \emptyset$, share exactly one vertex or have one edge in common. Denote a finite element (K, P_K, D_K) by Ciarlet's triple [5], the subscription K implying the dependence of the quadrilateral K . Let \mathcal{N}_h denote the set of all the vertexes, $\mathcal{N}_h = \mathcal{N}_h^i \cup \mathcal{N}_h^b$, with \mathcal{N}_h^i and \mathcal{N}_h^b consisting of the interior vertexes and the boundary vertexes, respectively. Similarly, let $\mathcal{E}_h = \mathcal{E}_h^i \cup \mathcal{E}_h^b$ denote the set of all the edges, with \mathcal{E}_h^i and \mathcal{E}_h^b consisting of the interior edges and the boundary edges, respectively. The subscript h in various notations implies the dependence of the subdivision. Denote by h_K the diameter of each quadrilateral K and the grid size $h \triangleq \max_{K \in \mathcal{J}_h} h_K$. On the edge e , we use $[\![\cdot]\!]_e$ for the jump across e .

Throughout the paper we denote by C a positive constant not necessarily the same at each occurrence but always independent of the diameter h_K or the grid size h . Denote $\lambda_{F,G}$ by the

generalized eigenvalue of matrix pair (F, G) , i.e., $F\mathbf{x} = \lambda_{F,G}G\mathbf{x}$. We use notations P_e and P_K to denote the average of the integral on the edge e and quadrilateral K , respectively.

2. GEOMETRY OF THE QUADRILATERALS

2.1. Quadrilateral and functions. Let K be a convex quadrilateral with A_i the vertices and e_i the edges, $i = 1 : 4$, see Figure 1. Let m_i be the mid-point of e_i , then the quadrilateral $\square m_1 m_2 m_3 m_4$ is a parallelogram. The cross point of $m_1 m_3$ and $m_2 m_4$, which is labelled as O , is the midpoint of both $m_1 m_3$ and $m_2 m_4$. Denote $r = \overrightarrow{Om_4}$ and $s = \overrightarrow{Om_1}$. Then, the coordinates of the vertices in the coordinate system rOs are $A_1(1+\alpha, 1+\beta)$, $A_2(-1-\alpha, 1-\beta)$, $A_3(-1+\alpha, -1+\beta)$, $A_4(1-\alpha, -1-\beta)$ and for some α, β . Since K is convex, $|\alpha| + |\beta| < 1$. Without loss of generality, we assume $\alpha > 0, \beta > 0$ and $r \times s > 0$. Here and after, we call α, β local shape parameters.

Define the shape regularity indicator of the quadrilateral K by $\mathcal{R}_K = \max\{\frac{|r||s|}{r \times s}, \frac{|r|}{|s|}, \frac{|s|}{|r|}\}$. Ev-

idently $\mathcal{R}_K \geq 1$, and $\mathcal{R}_K = 1$ if and only if K is a square. A given family of quadrilateral subdivisions $\{\mathcal{J}_h\}$ of Ω is called regular, if all the shape regularity indicators of the quadrilaterals of all the subdivisions are uniformly bounded.

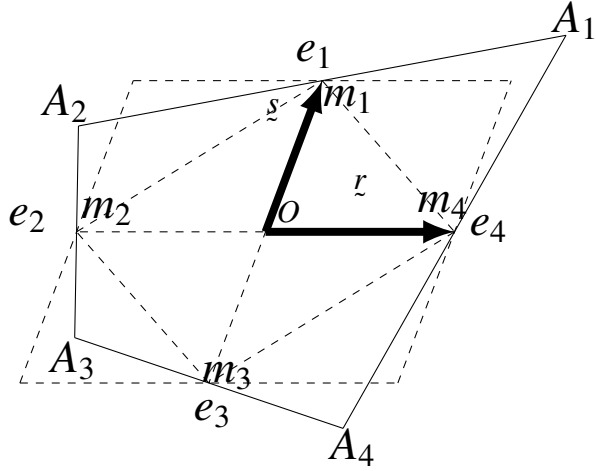


FIGURE 1. Illustration of a convex quadrilateral K .

Define two linear functions ξ and η by $\xi(ar + bs) = a$ and $\eta(ar + bs) = b$. The two functions play the same role on quadrilaterals as that played by barycentric coordinates on triangles. Additionally we also define two functions $\hat{\xi}$ and $\hat{\eta}$ by $\hat{\xi} = \xi - \int_K \xi \, dx$, $\hat{\eta} = \eta - \int_K \eta \, dx$ for convenience of calculation in Section 4. Technically, we construct two tables about the evaluation of some functions which will be useful in theoretical analysis and numerical computation.

TABLE 1. boundary integral evaluation of some functions

Function	ξ^2	$\xi\eta$	η^2
\int_{e_1}	$\frac{(1+\alpha)^2 e_1 }{3}$	$\frac{(1+\alpha)\beta e_1 }{3}$	$\frac{(3+\beta^2) e_1 }{3}$
\int_{e_2}	$\frac{(3+\alpha^2) e_2 }{3}$	$\frac{\alpha(-1+\beta) e_2 }{3}$	$\frac{(1-\beta)^2 e_2 }{3}$
\int_{e_3}	$\frac{(1-\alpha)^2 e_3 }{3}$	$\frac{(-1+\alpha)\beta e_3 }{3}$	$\frac{(3+\beta^2) e_3 }{3}$
\int_{e_4}	$\frac{(3+\alpha^2) e_4 }{3}$	$\frac{\alpha(1+\beta) e_4 }{3}$	$\frac{(1+\beta)^2 e_4 }{3}$

TABLE 2. integral evaluation of some functions in domain K

Function	1	ξ	η	ξ^2	$\xi\eta$	η^2
\int_K	$4\mathcal{L} \times \mathcal{S}$	$\frac{4\beta}{3}\mathcal{L} \times \mathcal{S}$	$\frac{4\alpha}{3}\mathcal{L} \times \mathcal{S}$	$\frac{4}{3}(1+\alpha^2)\mathcal{L} \times \mathcal{S}$	$\frac{4}{3}a\beta\mathcal{L} \times \mathcal{S}$	$\frac{4}{3}(1+\beta^2)\mathcal{L} \times \mathcal{S}$
Function	1	$\hat{\xi}$	$\hat{\eta}$	$\hat{\xi}^2$	$\hat{\xi}\hat{\eta}$	$\hat{\eta}^2$
\int_K	$4\mathcal{L} \times \mathcal{S}$	0	0	$\frac{4}{9}(3+3\alpha^2-\beta^2)\mathcal{L} \times \mathcal{S}$	$\frac{8}{9}a\beta\mathcal{L} \times \mathcal{S}$	$\frac{4}{9}(3+3\beta^2-\alpha^2)\mathcal{L} \times \mathcal{S}$

2.2. Grid refinement. Denote by d_K the distance between the midpoints of the diagonals of the quadrilateral K , then we introduce a lemma.

Lemma 1. *All refined quadrilaterals produced by a bisection scheme of grid subdivisions have the property $d_K = O(h_K^2)$.*

Proof. The proof can be found in [13, 16]. □

Here and after, we call the grid generated by the bisection scheme as an asymptotically parallel grid. We notice that the quantity $\max_{K \in \mathcal{J}_h} \{\alpha_K, \beta_K\}$ is of order $O(h)$ uniformly for asymptotically regular parallelogram grid by Lemma 1. This proposition will be used frequently in the Section 4.

2.3. On the construction of conforming element with piecewise polynomials. Hereby, we prove that, as rigorously presented in the below theorem, for general quadrilateral grids, no practically useful conforming elements can be constructed with piecewise polynomials.

Theorem 2. *Let $\text{FEM}_{pq} = (K, P_K, N_K)$ be a finite element defined by Ciarlet's triple, with K being any quadrilateral, and P_K being a space of polynomials on K . If the finite element space generated by FEM_{pq} by the continuity of nodal parameters is an H^1 subspace on any grid that consists of arbitrary quadrilaterals, then P_K only contains polynomials that vanish on the boundary of K .*

Remark 3. *Shortly speaking, if a finite element FEM_{pq} , the subscripts “ p ” for polynomial and “ q ” for quadrilateral, can formulate continuous piecewise polynomial space on general quadrilateral grids, then the shape function space of the finite element consists of bubble functions on*

K only. This theorem shows the non-existence of practically useful conforming finite element defined by Ciarlet's triple on general quadrilateral grids. However, we emphasize that it does not exclude the possibility that, on a given quadrilateral grid, a subspace of $H_0^1(\Omega)$ that consists of piecewise k -th degree polynomials can contain more than cell bubbles.

Proof of Theorem 2. By the assumption that FEM_{pq} can formulate an H^1 subspace on a grid that consists of arbitrary quadrilaterals, given a quadrilateral K_1 with D being one of its vertices, without loss of generality, we assume there is a shape function (polynomial) q defined on K_1 , such that $q = 0$ along the two edges of which D is **not** an endpoint and q is nontrivial along one edge $e \ni D$ of K_1 . By the continuity of the finite element space generated from FEM_{pq} by the continuity of nodal parameters and by the arbitrariness of choosing the evaluation of nodal parameters, for any groups of quadrilaterals (including K_1) which can form a patch ω_D centered at D (see Figure 2 for a reference), there exists a finite element function $r \in H_0^1(\omega_D)$, such that $r|_{K_1} = q$. Again, we emphasize that the evaluation on these common nodal parameters do not inflect the evaluation of the finite element function on the edges which do not intersect with K_1 , and this is why r can be chosen in $H_0^1(\omega_D)$.

Now, since $r|_f = 0$, we can rewrite $r|_{K_2} = r_{-1} \cdot l_f$, where l_f is a first degree polynomial which vanishes on f and r_{-1} is a polynomial with one degree lower than r . Without loss of generality, we assume f is not parallel to e . By the continuity of r on e , we can rewrite $q|_e = q_{-1}l_f|_e = q_{-1}(t - \theta)$, where t is the length parameter of e , q_{-1} is a polynomial on e with one degree lower than q and θ varies as the angle between e and f varies. Recall that K_1 and q_{K_1} are fixed, but f can be arbitrary. Change f to another direction f' , by elementary calculation, it follows that $q|_e = q_{-2}(t - \theta)(t - \theta')$. This way, by repeating the procedure, we can see that $q|_e$ contains a polynomial factor with growing degree and thus can not be a nontrivial polynomial. This leads to a contradiction to the assumption that $q|_e \not\equiv 0$ and completes the proof. \square

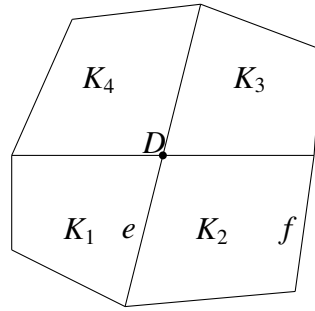


FIGURE 2. The patch ω_D around K_1 centered at D .

Remark 4. Similarly, conforming finite elements can not be defined for $H(\text{rot})$ with piecewise polynomials for general quadrilateral grids. Indeed, the assertion can be generalized to general Sobolev spaces.

3. A SEQUENCE OF LOWEST-DEGREE FINITE ELEMENTS

3.1. Definitions of the finite elements. In the subsection we introduce three types of finite elements.

The quadrilateral finite element presented below is similar to the bilinear element on rectangle, and we call it the quadrilateral bilinear (QBL) element.

The QBL element is defined by $(K, P_K^{\text{QBL}}, D_K^{\text{QBL}})$ with

1. K is a convex quadrilateral with vertexes $A_i, i = 1 : 4$
2. $P_K^{\text{QBL}} \triangleq \text{span}\{1, \xi, \eta, \xi\eta\}$
3. $D_K^{\text{QBL}} \triangleq \{u(A_i), i = 1 : 4\} \quad \text{for any } u \in H^2(K)$

QBL element defined above is unisolvant. Indeed, define

(2)

$$\left\{ \begin{array}{l} \phi_1 = \frac{\alpha + \beta - 1}{4(\alpha^2 + \beta^2 - 1)} \xi \eta + \frac{(\beta - 1)(-\alpha + \beta + 1)}{4(\alpha^2 + \beta^2 - 1)} \xi + \frac{(\alpha - 1)(\alpha - \beta + 1)}{4(\alpha^2 + \beta^2 - 1)} \eta + \frac{-(\alpha - 1)(\beta - 1)(\alpha + \beta + 1)}{4(\alpha^2 + \beta^2 - 1)} \\ \phi_2 = \frac{-\alpha + \beta + 1}{4(\alpha^2 + \beta^2 - 1)} \xi \eta + \frac{-(\beta + 1)(\alpha + \beta - 1)}{4(\alpha^2 + \beta^2 - 1)} \xi + \frac{(\alpha - 1)(\alpha + \beta + 1)}{4(\alpha^2 + \beta^2 - 1)} \eta + \frac{(\alpha - 1)(\beta + 1)(\alpha - \beta + 1)}{4(\alpha^2 + \beta^2 - 1)} \\ \phi_3 = \frac{-(\alpha + \beta + 1)}{4(\alpha^2 + \beta^2 - 1)} \xi \eta + \frac{(\beta + 1)(\alpha - \beta + 1)}{4(\alpha^2 + \beta^2 - 1)} \xi + \frac{(\alpha + 1)(-\alpha + \beta + 1)}{4(\alpha^2 + \beta^2 - 1)} \eta + \frac{(\alpha + 1)(\beta + 1)(\alpha + \beta - 1)}{4(\alpha^2 + \beta^2 - 1)} \\ \phi_4 = \frac{\alpha - \beta + 1}{4(\alpha^2 + \beta^2 - 1)} \xi \eta + \frac{(\beta - 1)(\alpha + \beta + 1)}{4(\alpha^2 + \beta^2 - 1)} \xi + \frac{-(\alpha + 1)(\alpha + \beta - 1)}{4(\alpha^2 + \beta^2 - 1)} \eta + \frac{(\alpha + 1)(\beta - 1)(-\alpha + \beta + 1)}{4(\alpha^2 + \beta^2 - 1)}. \end{array} \right.$$

then we can verify directly $\phi_i(A_j) = \delta_{ij}, i, j = 1 : 4$.

Here and after, the functions $\{\phi_i\}_{i=1:4}$ are called local basis of P_K^{QBL} . We use the notation $\phi_i^{(j)}$ to denote j -th coefficient of i -th basis, for example, $\phi_1^{(2)} = \frac{(\beta-1)(-\alpha+\beta+1)}{4(\alpha^2+\beta^2-1)}$.

Given a QBL element $(K, P_K^{\text{QBL}}, D_K^{\text{QBL}})$, define the local interpolation operator J_K by

$$(3) \quad J_K u = \sum_{i=1}^4 u(A_i) \phi_i, \quad \forall u \in H^2(K).$$

Furthermore, given a family of QBL elements $(K_i, P_{K_i}^{\text{QBL}}, D_{K_i}^{\text{QBL}})$ in a subdivision \mathcal{J}_h , define the global interpolation operator J_h by

$$(4) \quad J_h u|_{K_i} = J_{K_i} u \quad \forall K_i \in \mathcal{J}_h.$$

The quadrilateral finite element presented below is similar to the Raviart-Thomas element on rectangle, and we call it the quadrilateral Raviart-Thomas (QRT) element.

The QRT element is defined by $(K, P_K^{\text{QRT}}, D_K^{\text{QRT}})$ with

1. K is a convex quadrilateral with edges $e_i, i = 1 : 4$
2. $P_K^{\text{QRT}} \triangleq \text{span}\{\nabla\xi, \nabla\eta, \xi\nabla\eta, \eta\nabla\xi\}$
3. $D_K^{\text{QRT}} \triangleq \{\int_{e_i} \varphi \cdot t_i \, ds, i = 1 : 4\} \quad \text{for any } \varphi \in H^1(K)$

Here t_i is the unit tangential vector of e_i respectively and the positive direction is counterclockwise along ∂K .

The QRT element as above is unisolvant. Indeed, define

(5)

$$\left\{ \begin{array}{l} \tilde{\phi}_1 = \frac{(1-\alpha)(1-\beta^2)|e_1|}{4(\alpha^2+\beta^2-1)} \nabla\xi + \frac{\alpha(1-\alpha)\beta|e_1|}{4(\alpha^2+\beta^2-1)} \nabla\eta + \frac{-\alpha(1-\alpha)|e_1|}{4(\alpha^2+\beta^2-1)} \xi\nabla\eta + \frac{(1-\alpha-\beta^2)|e_1|}{4(\alpha^2+\beta^2-1)} \eta\nabla\xi \\ \tilde{\phi}_2 = \frac{\alpha\beta(1+\beta)|e_2|}{4(\alpha^2+\beta^2-1)} \nabla\xi + \frac{(1-\alpha^2)(1+\beta)|e_2|}{4(\alpha^2+\beta^2-1)} \nabla\eta + \frac{-(1-\alpha^2+\beta)|e_2|}{4(\alpha^2+\beta^2-1)} \xi\nabla\eta + \frac{-\beta(1+\beta)|e_2|}{4(\alpha^2+\beta^2-1)} \eta\nabla\xi \\ \tilde{\phi}_3 = \frac{-(1+\alpha)(1-\beta^2)|e_3|}{4(\alpha^2+\beta^2-1)} \nabla\xi + \frac{-\alpha(1+\alpha)\beta|e_3|}{4(\alpha^2+\beta^2-1)} \nabla\eta + \frac{\alpha(1+\alpha)|e_3|}{4(\alpha^2+\beta^2-1)} \xi\nabla\eta + \frac{(1+\alpha-\beta^2)|e_3|}{4(\alpha^2+\beta^2-1)} \eta\nabla\xi \\ \tilde{\phi}_4 = \frac{-\alpha\beta(1-\beta)|e_4|}{4(\alpha^2+\beta^2-1)} \nabla\xi + \frac{-(1-\alpha^2)(1-\beta)|e_4|}{4(\alpha^2+\beta^2-1)} \nabla\eta + \frac{-(1-\alpha^2-\beta)|e_4|}{4(\alpha^2+\beta^2-1)} \xi\nabla\eta + \frac{\beta(1-\beta)|e_4|}{4(\alpha^2+\beta^2-1)} \eta\nabla\xi. \end{array} \right.$$

Denote $\{D_i^{\text{QRT}}\}_{i=1:4}$ by the components of D_K^{QRT} , then we can verify directly $D_i^{\text{QRT}}(\tilde{\phi}_j) = \delta_{ij}$, $i, j = 1 : 4$.

Here and after, the functions $\{\tilde{\phi}_i\}_{i=1:4}$ are called local basis of P_K^{QRT} .

Given the QRT element $(K, P_K^{\text{QRT}}, D_K^{\text{QRT}})$, define the local interpolation operator \square_K by

$$(6) \quad \square_K \varphi = \sum_{i=1}^4 D_i^{\text{QRT}}(\varphi) \tilde{\phi}_i \quad \forall \varphi \in H^1(K).$$

Furthermore, given a family of QRT elements $(K_i, P_{K_i}^{\text{QRT}}, D_{K_i}^{\text{QRT}})$ in a subdivision \mathcal{J}_h , define the global interpolation operator \square_h by

$$(7) \quad \square_h \varphi|_{K_i} = \square_{K_i} \varphi \quad \forall K_i \in \mathcal{J}_h.$$

Finally, for any $q \in L^2(\Omega)$ define the interpolation operator P_h by $P_h q|_{K_i} = P_{K_i} q, \forall K_i \in \mathcal{J}_h$.

3.1.1. Exact sequences on a quadrilateral.

Theorem 5. *The commutative diagram holds as below:*

$$\begin{array}{ccccccc}
 \mathbb{R} & \longrightarrow & H^2(K) & \xrightarrow{\nabla} & \mathcal{H}^1(K) & \xrightarrow{\text{rot}} & L^2(K) & \xrightarrow{\int_K \cdot} & \mathbb{R} \\
 & & \downarrow J_K & & \downarrow \square_K & & \downarrow P_K & & \\
 \mathbb{R} & \longrightarrow & P_K^{\text{QBL}} & \xrightarrow{\nabla} & P_K^{\text{QRT}} & \xrightarrow{\text{rot}} & \mathbb{R} & \xrightarrow{\int_K \cdot} & \mathbb{R}.
 \end{array}$$

Proof. We first prove the discretized de Rham complex. Evidently $\ker(\nabla) = \mathbb{R}$ and $\nabla P_K^{\text{QBL}} \subset P_K^{\text{QRT}}$. On the other hand, $\text{rot} P_K^{\text{QRT}} = \mathbb{R}$. It remains to prove that $\ker(\text{rot}) = \nabla P_K^{\text{QBL}}$. Given a $\underline{\tau} \in P_K^{\text{QRT}}$, such that $\text{rot} \underline{\tau} = 0$. Since $\underline{\tau} = d_1 \nabla \xi + d_2 \nabla \eta + d_3 \xi \nabla \eta + d_4 \eta \nabla \xi$, then we have $d_3 = d_4$ and $\underline{\tau} \in \nabla P_K^{\text{QBL}}$.

Then we are going to show that $\nabla J_K = \square_K \nabla$ on $H^2(K)$, and $\text{rot} \square_K = P_K \text{rot}$ on $\mathcal{H}^1(K)$. We first prove the former. Given a $\underline{\sigma} \in \mathcal{H}^1(K)$, let $\square_K \underline{\sigma} = g_1 \cdot \nabla \xi + g_2 \cdot \nabla \eta + g_3 \cdot \xi \nabla \eta + g_4 \cdot \eta \nabla \xi$. By definition, we have

$$\begin{aligned}
 g_1 &= \frac{(1-\alpha)(1-\beta^2)\underline{\varepsilon}_1 \cdot P_{e_1}(\underline{\sigma}) + \alpha\beta(1+\beta)\underline{\varepsilon}_2 \cdot P_{e_2}(\underline{\sigma}) - (1+\alpha)(1-\beta^2)\underline{\varepsilon}_3 \cdot P_{e_3}(\underline{\sigma}) - \alpha\beta(1-\beta)\underline{\varepsilon}_4 \cdot P_{e_4}(\underline{\sigma})}{4(\alpha^2 + \beta^2 - 1)} \\
 g_2 &= \frac{\alpha(1-\alpha)\beta\underline{\varepsilon}_1 \cdot P_{e_1}(\underline{\sigma}) + (1-\alpha^2)(1+\beta)\underline{\varepsilon}_2 \cdot P_{e_2}(\underline{\sigma}) - \alpha(1+\alpha)\beta\underline{\varepsilon}_3 \cdot P_{e_3}(\underline{\sigma}) - (1-\alpha^2)(1-\beta)\underline{\varepsilon}_4 \cdot P_{e_4}(\underline{\sigma})}{4(\alpha^2 + \beta^2 - 1)} \\
 g_3 &= \frac{-\alpha(1-\alpha)\underline{\varepsilon}_1 \cdot P_{e_1}(\underline{\sigma}) - (1-\alpha^2 + \beta)\underline{\varepsilon}_2 \cdot P_{e_2}(\underline{\sigma}) + \alpha(1+\alpha)\underline{\varepsilon}_3 \cdot P_{e_3}(\underline{\sigma}) - (1-\alpha^2 - \beta)\underline{\varepsilon}_4 \cdot P_{e_4}(\underline{\sigma})}{4(\alpha^2 + \beta^2 - 1)} \\
 g_4 &= \frac{(1-\alpha-\beta^2)\underline{\varepsilon}_1 \cdot P_{e_1}(\underline{\sigma}) - \beta(1+\beta)\underline{\varepsilon}_2 \cdot P_{e_2}(\underline{\sigma}) + (1+\alpha-\beta^2)\underline{\varepsilon}_3 \cdot P_{e_3}(\underline{\sigma}) + \beta(1-\beta)\underline{\varepsilon}_4 \cdot P_{e_4}(\underline{\sigma})}{4(\alpha^2 + \beta^2 - 1)}.
 \end{aligned}$$

Now given a $u \in H^2(K)$, we take $\underline{\sigma} = \nabla u \in \mathcal{H}^1(K)$ and the former follows by simple calculation.

It remains to prove the latter. Since $\nabla \xi = \frac{s^\perp}{\underline{\ell} \times \underline{s}}$, $\nabla \eta = \frac{r^\perp}{\underline{\ell} \times \underline{s}}$, then for $\underline{\sigma} \in \mathcal{H}^1(K)$ it holds

$$\text{rot}(\square_K \underline{\sigma}) = (g_3 - g_4) \nabla \xi \times \nabla \eta = \frac{g_3 - g_4}{r \times s} = \frac{1}{4r \times s} \int_{\partial K} \underline{\sigma} \cdot \underline{t} \, ds = P_K(\text{rot} \underline{\sigma}).$$

The proof is completed. \square

3.2. Interpolation error estimation.

3.2.1. Interpolation error estimations in L^2 norm.

Theorem 6. *Let K be a convex quadrilateral, then it holds*

$$\|u - J_K u\|_{0,K} \leq Ch_K^2 |u|_{2,K} \quad \forall u \in H^2(K).$$

Proof. By density, it suffices to consider $u \in C^2(\bar{K})$. Let A be any point in the quadrilateral K with vertexes $\{A_i\}_{i=1:4}$. Using Taylor expansion with integral remainder, we have

$$u(A_i) = u(A) + \nabla u(A) \cdot (A_i - A) + R_i(A), \quad R_i(A) = \int_0^1 (1-t) \frac{d^2 u}{dt^2}(\xi_i, \eta_i) dt.$$

Here $\xi_i = tx_i + (1-t)x$, $\eta_i = ty_i + (1-t)y$.

Since J_K preserves linear polynomial

$$J_K u(A) = \sum_{i=1}^4 u(A_i) \phi_i(A) = u(A) + \sum_{i=1}^4 R_i(A) \phi_i(A).$$

Then we obtain

$$u(A) - J_K u(A) = - \sum_{i=1}^4 R_i(A) \phi_i(A).$$

Evidently

$$\begin{aligned} |R_i(A)|^2 &= \left| \int_0^1 (1-t) \left(\frac{\partial^2 u}{\partial \xi_i^2} (x_i - x)^2 + 2 \frac{\partial^2 u}{\partial \xi_i \partial \eta_i} (x_i - x)(y_i - y) + \frac{\partial^2 u}{\partial \eta_i^2} (y_i - y)^2 \right) dt \right|^2 \\ &\leq 4h_K^4 \int_0^1 (1-t)^2 \sum_{|m|=2} |\partial^m u(\xi_i, \eta_i)|^2 dt \\ \|u - J_K u\|_{0,K}^2 &\leq Ch_K^4 \sum_{i=1}^4 \sum_{|m|=2} \int_0^1 (1-t)^2 \int_K |\partial^m u(\xi_i, \eta_i)|^2 dx dy dt. \end{aligned}$$

Take integral variable substitution: $d\xi_i = (1-t)dx$, $d\eta_i = (1-t)dy$, then we have

$$\|u - J_K u\|_{0,K}^2 \leq Ch_K^4 \sum_{i=1}^4 \sum_{|m|=2} \int_0^1 \int_K |\partial^m u(\xi_i, \eta_i)|^2 d\xi_i d\eta_i dt = Ch_K^4 |u|_{2,K}^2.$$

The proof is completed. \square

Theorem 7. *Let K be a convex quadrilateral, then it holds*

$$(8) \quad \|\underline{\sigma} - \square_K \underline{\sigma}\|_{0,K} \leq Ch_K |\underline{\sigma}|_{1,K} \quad \forall \underline{\sigma} \in H^1(K).$$

We postpone the proof of the theorem after a technical lemma. Define a new interpolation operator $\square_Q : \underline{H}^1(K) \rightarrow \text{span}\{1, \xi, \eta, \xi^2 - \eta^2\}$ by $\int_{e_i} \underline{\sigma} \, ds = \int_{e_i} \square_Q \underline{\sigma} \, ds, i = 1 : 4$. Evidently \square_Q is well-defined.

Lemma 8. *The local interpolation operator \square_K is H^1 stable, namely*

$$|\square_K \underline{\sigma}|_{1,K} \leq C |\underline{\sigma}|_{1,K} \quad \forall \underline{\sigma} \in \underline{H}^1(K).$$

Proof. Let $\square_Q \underline{\sigma} = \underline{d}_1 \cdot 1 + \underline{d}_2 \cdot \xi + \underline{d}_3 \cdot \eta + \underline{d}_4 \cdot (\xi^2 - \eta^2)$, then by definition we have

$$\begin{aligned} \underline{d}_1 &= \frac{\alpha^2 - \beta^2 + 2}{8} P_{e_1}(\underline{\sigma}) + \frac{-\alpha^2 + \beta^2 + 2}{8} P_{e_2}(\underline{\sigma}) + \frac{\alpha^2 - \beta^2 + 2}{8} P_{e_3}(\underline{\sigma}) + \frac{-\alpha^2 + \beta^2 + 2}{8} P_{e_4}(\underline{\sigma}) \\ \underline{d}_2 &= -\frac{\beta}{4} P_{e_1}(\underline{\sigma}) + \frac{\beta - 2}{4} P_{e_2}(\underline{\sigma}) - \frac{\beta}{4} P_{e_3}(\underline{\sigma}) + \frac{\beta + 2}{4} P_{e_4}(\underline{\sigma}) \\ \underline{d}_3 &= \frac{\alpha + 2}{4} P_{e_1}(\underline{\sigma}) - \frac{\alpha}{4} P_{e_2}(\underline{\sigma}) + \frac{\alpha - 2}{4} P_{e_3}(\underline{\sigma}) - \frac{\alpha}{4} P_{e_4}(\underline{\sigma}) \\ \underline{d}_4 &= -\frac{3}{8} P_{e_1}(\underline{\sigma}) + \frac{3}{8} P_{e_2}(\underline{\sigma}) - \frac{3}{8} P_{e_3}(\underline{\sigma}) + \frac{3}{8} P_{e_4}(\underline{\sigma}). \end{aligned}$$

Denote by row vector $\underline{\sigma} = (\sigma_1, \sigma_2)$, $\underline{p}_1 = (P_{e_i}(\sigma_1))_{i=1:4}$, $\underline{p}_2 = (P_{e_i}(\sigma_2))_{i=1:4}$, and column vector $\underline{p} = (\underline{p}_1, \underline{p}_2)^T$. Denote \equiv by = up to a constant, independent of diameter h_K , then

$$\begin{aligned} \int_K |\nabla(\square_Q \underline{\sigma})|^2 \, dx &\equiv h_K^{-2} \int_K |\partial_\xi(\square_Q \underline{\sigma})|^2 + |\partial_\eta(\square_Q \underline{\sigma})|^2 \, dx = h_K^{-2} \int_K |\underline{d}_2 + 2\underline{d}_4 \xi|^2 + |\underline{d}_3 - 2\underline{d}_4 \eta|^2 \, dx \\ &\equiv |\underline{d}_2|^2 + |\underline{d}_3|^2 + |\underline{d}_4|^2 = \underline{p}_1^T B_1^T B_1 \underline{p}_1^T + \underline{p}_2^T B_1^T B_1 \underline{p}_2^T = \underline{p}^T B \underline{p}. \end{aligned}$$

Here $\underline{p} \in \mathbb{R}^8$ and

$$B_1 = \begin{bmatrix} -\frac{\beta}{4} & -\frac{\beta-2}{4} & -\frac{\beta}{4} & \frac{\beta+2}{4} \\ \frac{\alpha+2}{4} & -\frac{\alpha}{4} & \frac{\alpha-2}{4} & -\frac{\alpha}{4} \\ -\frac{3}{8} & \frac{3}{8} & -\frac{3}{8} & \frac{3}{8} \end{bmatrix}, \quad B = \begin{bmatrix} B_1^T B_1 & 0 \\ 0 & B_1^T B_1 \end{bmatrix}.$$

Similarly, let $\square_K \underline{\sigma} = g_1 \cdot \nabla \xi + g_2 \cdot \nabla \eta + g_3 \cdot \xi \nabla \eta + g_4 \cdot \eta \nabla \xi$, recalling $\{g_i\}_{i=1:4}$ in Theorem 5, then there exists a semi-positive matrix D with $O(1)$ elements such that $|\square_K \underline{\sigma}|_{1,K}^2 = \underline{p}^T D \underline{p}$.

Since \square_Q is H^1 stable (see [15]), it remains to show that $|\square_K \underline{\sigma}|_{1,K} \leq C |\square_Q \underline{\sigma}|_{1,K}$.

We first show that $\ker B \subset \ker D$. Given a $\tilde{p} \in \ker B$, then $|\nabla_Q \tilde{\sigma}|_{1,K}^2 = 0$ and $\nabla_Q \tilde{\sigma}$ is a constant vector. Since $\nabla_K \tilde{\sigma} = \nabla_K(\nabla_Q \tilde{\sigma})$, thus $\nabla_K \tilde{\sigma}$ is also a constant vector and $|\nabla_K \tilde{\sigma}|_{1,K}^2 = 0$, i.e. $\tilde{p} \in \ker D$.

Subsequently, we calculate all the eigenvalues of $B_1^T B_1$, (below we use $\lambda_i = \lambda_i(B_1^T B_1)$, $i = 1 : 4$)

$$\begin{aligned} \lambda_1 &= 0 & \lambda_3 &= \frac{17}{32} + \frac{\alpha^2 + \beta^2}{8} - \frac{\sqrt{16(\alpha^4 + \beta^4) + 32\alpha^2\beta^2 + 136(\alpha^2 + \beta^2) + 1}}{32} \\ \lambda_2 &= \frac{1}{2} & \lambda_4 &= \frac{17}{32} + \frac{\alpha^2 + \beta^2}{8} + \frac{\sqrt{16(\alpha^4 + \beta^4) + 32\alpha^2\beta^2 + 136(\alpha^2 + \beta^2) + 1}}{32}. \end{aligned}$$

The eigenvalues $\lambda(B) = \{\lambda_1, \lambda_2, \lambda_3, \lambda_4\}$ of matrix B are all double eigenvalues. Let $\{\tilde{\gamma}_1, \tilde{\gamma}_2\}$ be two eigenvectors subordinating to the eigenvalue $\lambda_1 = 0$. Then we can decompose $\mathbb{R}^8 = \text{span}\{\tilde{\gamma}_1, \tilde{\gamma}_2\} \oplus (\text{span}\{\tilde{\gamma}_1, \tilde{\gamma}_2\})^\perp$. Suppose $\tilde{p} = \tilde{\psi}_1 + \tilde{\psi}_2$, $\tilde{\psi}_1 \in \text{span}\{\tilde{\gamma}_1, \tilde{\gamma}_2\}$, $\tilde{\psi}_2 \in (\text{span}\{\tilde{\gamma}_1, \tilde{\gamma}_2\})^\perp$.

Rayleigh quotient theorem reads

$$|\nabla_K \tilde{\sigma}|_{1,K}^2 = \tilde{p}^T D \tilde{p} = \tilde{\psi}_2^T D \tilde{\psi}_2 \leq \lambda_{\max}(D) |\tilde{\psi}_2|^2$$

$$|\nabla_Q \tilde{\sigma}|_{1,K}^2 = \tilde{p}^T B \tilde{p} = \tilde{\psi}_2^T B \tilde{\psi}_2 \geq \min\{\lambda_2, \lambda_3, \lambda_4\} |\tilde{\psi}_2|^2.$$

This finishes the proof. \square

Proof of Theorem 7. Dividing a quadrilateral K along the diameter into two triangles, we have the following estimation from the similar argument referred to Theorem 5.1 in [4].

$$\|\tilde{\sigma} - \nabla_K \tilde{\sigma}\|_{0,K} \leq Ch_K \|\nabla(\tilde{\sigma} - \nabla_K \tilde{\sigma})\|_{0,K}.$$

This proves (8) by Lemma 8.

Theorem 9. *Let K be a convex quadrilateral, then it holds*

$$\|q - P_K q\|_{0,K} \leq Ch_K |q|_{1,K} \quad \forall q \in H^1(K).$$

Proof. The proof can be found in [10]. \square

3.2.2. Interpolation error estimations in energy norms.

Theorem 10. *Let K be a convex quadrilateral, then it holds*

$$(9) \quad |u - J_K u|_{1,K} \leq Ch_K |u|_{2,K} \quad \forall u \in H^2(K),$$

and

$$(10) \quad |\tilde{\sigma} - \square_K \tilde{\sigma}|_{\text{rot}, K} \leq C h_K |\text{rot} \tilde{\sigma}|_{1, K} \quad \forall \tilde{\sigma} \in H^1(\text{rot}, K).$$

Proof. We prove the estimations by the commutative diagrams. Since $\nabla(J_K) = \square_K(\nabla)$ on $H^2(K)$, we have

$$|u - J_K u|_{1, K} = \|\nabla u - \square_K(\nabla u)\|_{0, K} \leq C h_K |u|_{2, K}.$$

Similarly, since $\text{rot} \square_K = P_K \text{rot}$ on $H^1(K)$, we have

$$\|\text{rot} \tilde{\sigma} - \text{rot}(\square_K \tilde{\sigma})\|_{0, K} = \|\text{rot} \tilde{\sigma} - P_K(\text{rot} \tilde{\sigma})\|_{0, K} \leq C h_K |\text{rot} \tilde{\sigma}|_{1, K}.$$

The proof is completed. \square

3.3. Finite element spaces on a grid \mathcal{T}_h .

Definition 11. Associated with the QBL element, define the finite element spaces V_h^{QBL} and V_{h0}^{QBL} by

$$V_h^{\text{QBL}} \triangleq \{v_h \in L^2(\Omega) : v_h|_K \in P_K^{\text{QBL}}, v_h \text{ is continuous at two endpoints of edge } e \in \mathcal{E}_h^i\},$$

$$\text{and } V_{h0}^{\text{QBL}} \triangleq \{v_h \in V_h^{\text{QBL}} : v_h = 0 \text{ at two endpoints of edge } e \in \mathcal{E}_h^b\}.$$

Definition 12. Associated with the QRT element, define the finite element spaces V_h^{QRT} and V_{h0}^{QRT} by

$$V_h^{\text{QRT}} \triangleq \{\underline{\tau}_h \in L^2(\Omega) : \underline{\tau}_h|_K \in P_K^{\text{QRT}}, \int_e \underline{\tau}_h \cdot \underline{t}_e \, ds \text{ is continuous at the edge } e \in \mathcal{E}_h^i\},$$

$$\text{and } V_{h0}^{\text{QRT}} \triangleq \{\underline{\tau}_h \in V_h^{\text{QRT}} : \int_e \underline{\tau}_h \cdot \underline{t}_e \, ds = 0 \text{ at the edge } e \in \mathcal{E}_h^b\}.$$

Definition 13. Define the piecewise constant finite element spaces W_h and W_{h0} by

$$W_h \triangleq \{q_h \in L^2(\Omega) : q_h|_K = P_K q, q \in L^2(\Omega)\}, \quad \text{and } W_{h0} \triangleq \{q_h \in W_h : \int_{\Omega} q_h \, dx = 0\}.$$

The properties on a single cell can be generalized on a grid. We firstly adopt a lemma below.

Lemma 14. It holds on the subdivision that

$$(11) \quad \sup_{\underline{\tau}_h \in V_h^{\text{QRT}}} (\text{rot}_h \underline{\tau}_h, q_h) \geq C \|\underline{\tau}_h\|_{\text{rot}, h} \|q_h\|_{0, \Omega}, \quad \text{for any } q_h \in W_h,$$

and

$$(12) \quad \sup_{\mathcal{T}_h \in V_{h0}^{\text{QRT}}} (\text{rot}_h \mathcal{T}_h, q_h) \geq C \|\mathcal{T}_h\|_{\text{rot},h} \|q_h\|_{0,\Omega}, \quad \text{for any } q_h \in W_{h0}.$$

Proof. Given $q_h \in W_h$, there exists a $\mathcal{T} \in H^1(\Omega)$, such that $\text{rot} \mathcal{T} = q_h$, and $\|\mathcal{T}\|_{1,\Omega} \leq C \|q_h\|_{0,\Omega}$. Set $\mathcal{T}_h := \square_h \mathcal{T}$, then $\text{rot}_h \mathcal{T}_h = q_h$, and $\|\mathcal{T}_h\|_{\text{rot},h} \leq C \|\mathcal{T}\|_{1,\Omega}$. This proves (11). Similarly is (12) proved. \square

Theorem 15. *The commutative diagrams hold as below:*

$$(13) \quad \begin{array}{ccccccc} \mathbb{R} & \longrightarrow & H^2(\Omega) & \xrightarrow{\nabla} & H^1(\Omega) & \xrightarrow{\text{rot}} & L^2(\Omega) & \xrightarrow{\int_{\Omega} \cdot} & \mathbb{R} \\ & & \downarrow J_h & & \downarrow \square_h & & \downarrow P_h & & \\ \mathbb{R} & \longrightarrow & V_h^{\text{QBL}} & \xrightarrow{\nabla_h} & V_h^{\text{QRT}} & \xrightarrow{\text{rot}_h} & W_h & \xrightarrow{\int_{\Omega} \cdot} & \mathbb{R}, \end{array}$$

and

$$(14) \quad \begin{array}{ccccccc} \{0\} & \longrightarrow & H^2(\Omega) \cap H_0^1(\Omega) & \xrightarrow{\nabla} & H^1(\Omega) \cap H_0(\text{rot}, \Omega) & \xrightarrow{\text{rot}} & L_0^2(\Omega) & \xrightarrow{\int_{\Omega} \cdot} & \{0\} \\ & & \downarrow J_h & & \downarrow \square_h & & \downarrow P_h & & \\ \{0\} & \longrightarrow & V_{h0}^{\text{QBL}} & \xrightarrow{\nabla_h} & V_{h0}^{\text{QRT}} & \xrightarrow{\text{rot}_h} & W_{h0} & \xrightarrow{\int_{\Omega} \cdot} & \{0\}. \end{array}$$

Proof. We first consider (13). The commutativity is trivial by Theorem 5 and it remains us to verify the discretized de Rham complex by the standard dimension counting technique.

Evidently $\ker(\nabla_h) = \mathbb{R}$ and $\nabla_h V_h^{\text{QBL}} \subset V_h^{\text{QRT}}$. On the other hand, by (11), $\text{rot}_h V_h^{\text{QRT}} = W_h$. This way, (13) follows by noting that $\dim(V_h^{\text{QBL}}) = \#(\mathcal{N}_h)$ and $\dim(V_h^{\text{QRT}}) = \#(\mathcal{E}_h)$, and that $\dim(V_h^{\text{QRT}}) = \dim(V_h^{\text{QBL}}) + \dim(W_h) - 1$ by the Euler formula.

Similarly is (14) proved. The proof is completed. \square

The error estimation of the global interpolator is the same as that of the respective local ones.

Theorem 16. *There exists a constant C depending on the shape regularity of \mathcal{T}_h only, such that*

- (1) $\|u - J_h u\|_{0,\Omega} + h|u - J_h u|_{1,h} \leq C h^2 |u|_{2,\Omega} \quad \forall u \in H^2(\Omega);$
- (2) $\|\sigma - \square_h \sigma\|_{\text{rot},h} \leq C h (|\sigma|_{1,\Omega} + |\text{rot} \sigma|_{1,\Omega}) \quad \forall \sigma \in H^1(\text{rot}, \Omega);$
- (3) $\|q - P_h q\|_{0,\Omega} \leq C h |q|_{1,\Omega} \quad \forall q \in H^1(\Omega).$

4. NONCONFORMING FINITE ELEMENT SPACES AND THEIR MODULUS OF CONTINUITY

In this section, we show that on a grid that consists of arbitrary quadrilaterals and satisfies the condition that the cells are asymptotically parallelograms, the spaces V_h^{QBL} and V_h^{QRT} , though

not subspaces of H^1 and $H(\text{rot})$ respectively, the consistency can be controlled well. We begin with an analysis that V_h^{QBL} is in general not continuous.

4.1. Continuity and non-continuity of V_{h0}^{QBL} . Let \mathcal{G}_D be a patch with the center D and four cells K_1, K_2, K_3, K_4 , see Figure 3. Let $V_{h0}^{\text{QBL}}(\mathcal{G}_D)$ be QBL finite element space defined on \mathcal{G}_D with zero boundary condition. Denote by local shape parameters α_i, β_i of K_i , $i = 1 : 4$. Here $\alpha_i = \beta_i = 0$ for $i = 2 : 4$.

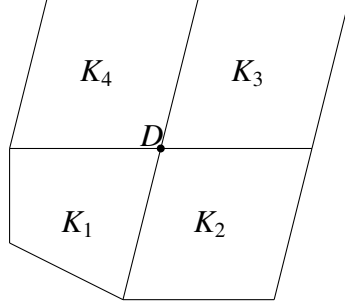


FIGURE 3. Illustration of a patch \mathcal{G}_D

Theorem 17. For $\alpha_1, \beta_1 \neq 0$ and $v_h \neq 0 \in V_{h0}^{\text{QBL}}(\mathcal{G}_D)$, there exists a function $\varphi \in C^\infty(\mathcal{G}_D)$ such that

$$(\nabla \varphi, \nabla_h v_h) + (\Delta \varphi, v_h) \neq 0$$

Proof. Since $\alpha_i, \beta_i = 0$ for $i = 2 : 4$, then

$$(\nabla \varphi, \nabla_h v_h) + (\Delta \varphi, v_h) = \int_{\partial K_1} \frac{\partial \varphi}{\partial n} (v_h - q) \, ds.$$

Here q is the linear interpolation of v_h on e with respect to endpoints. Without loss of generality, we assume $\alpha_1 \neq 0$. Noticing that $\dim V_{h0}^{\text{QBL}}(\mathcal{G}_D) = 1$, we denote by ϕ_D the basis of $V_{h0}^{\text{QBL}}(\mathcal{G}_D)$ and $\phi_D|_{K_1} = \phi_1$ (see (2)), then $v_h|_{K_1} = v_h(D)\phi_1$. Let φ be a linear polynomial whose gradient is $\mathcal{L}_{K_1}/\mathcal{L}_{K_1} \times \mathcal{L}_{K_1}$, defined on the patch \mathcal{G}_D . Then the proof is completed by simple calculation. \square

4.2. Modulus of continuity of V_{h0}^{QBL} . Define consistency functional $E(\zeta, v_h)$ by

$$(15) \quad E(\zeta, v_h) = (\zeta, \nabla_h v_h) + (\text{div} \zeta, v_h) \quad \text{for } \zeta \in \mathcal{H}^1(\Omega), v_h \in V_{h0}^{\text{QBL}}$$

$$(16) \quad E(\zeta, v_h) = (\zeta, \nabla_h v_h) + (\text{div} \zeta, v_h) \quad \text{for } \zeta \in \mathcal{H}_0^1(\Omega), v_h \in V_h^{\text{QBL}} \cap L_0^2(\Omega).$$

Let $\{\phi_i\}_{i=1:4}$ be local basis of P_K^{QBL} , then define by

$$\iota_1 = \sum_{i=1}^4 \phi_i^{(1)} v_h(A_i) \quad \iota_2 = \sum_{i=1}^4 \phi_i^{(2)} v_h(A_i) \quad \iota_3 = \sum_{i=1}^4 \phi_i^{(3)} v_h(A_i).$$

Theorem 18. For $\zeta \in \mathcal{H}^1(\Omega)$, $v_h \in V_{h0}^{\text{QBL}}$ or $\zeta \in \mathcal{H}_0^1(\Omega)$, $v_h \in V_h^{\text{QBL}}$, it holds

$$E(\zeta, v_h) \leq Ch \|\zeta\|_{1,\Omega} |v_h|_{1,h}.$$

Proof. Evidently the consistency functional can be decomposed into

$$E(\zeta, v_h) = \sum_{e \in \mathcal{E}_h} \int_e \zeta \cdot \eta_e [\![v_h - q]\!]_e \, ds = \sum_{K \in \mathcal{T}_h} \sum_{e \subset \partial K} \int_e \zeta \cdot \eta_e (v_h - q) \, ds.$$

Here q is the linear interpolation of v_h on e with respect to endpoints. Then by direct calculation, we have

$$\begin{aligned} \int_{\partial K} \zeta \cdot \eta (v_h - q) \, ds &= \beta_K \iota_1 \int_{e_1} \zeta \cdot \eta_1 \left(\frac{\xi^2}{1 + \alpha_K} - (1 + \alpha_K) \right) \, ds + \alpha_K \iota_1 \int_{e_2} \zeta \cdot \eta_2 \left(\frac{\eta^2}{-1 + \beta_K} - (-1 + \beta_K) \right) \, ds \\ &\quad + \beta_K \iota_1 \int_{e_3} \zeta \cdot \eta_3 \left(\frac{\xi^2}{-1 + \alpha_K} - (-1 + \alpha_K) \right) \, ds + \alpha_K \iota_1 \int_{e_4} \zeta \cdot \eta_4 \left(\frac{\eta^2}{1 + \beta_K} - (1 + \beta_K) \right) \, ds \\ &\leq Ch \iota_1 \|\zeta\|_{1,K}. \end{aligned}$$

On the other hand, setting $\underline{\iota} = (\iota_1, \iota_2, \iota_3)^T$ and $|v_h|_{1,K}^2 = \underline{\iota}^T G \underline{\iota}$, then

$$G = \begin{bmatrix} 4(1+\beta_K^2) \underline{S}_K \cdot \underline{S}_K - 8\alpha_K \beta_K \underline{L}_K \cdot \underline{S}_K + 4(1+\alpha_K^2) \underline{L}_K \cdot \underline{L}_K & 4\alpha_K \underline{S}_K \cdot \underline{S}_K - 4\beta_K \underline{L}_K \cdot \underline{S}_K & -4\alpha_K \underline{L}_K \cdot \underline{S}_K + 4\beta_K \underline{L}_K \cdot \underline{L}_K \\ \hline 3\underline{L}_K \times \underline{S}_K & 3\underline{L}_K \times \underline{S}_K & 3\underline{L}_K \times \underline{S}_K \\ \hline 4\alpha_K \underline{S}_K \cdot \underline{S}_K - 4\beta_K \underline{L}_K \cdot \underline{S}_K & 4\underline{S}_K \cdot \underline{S}_K & -4\underline{L}_K \cdot \underline{S}_K \\ \hline 3\underline{L}_K \times \underline{S}_K & \underline{L}_K \times \underline{S}_K & \underline{L}_K \times \underline{S}_K \\ \hline -4\alpha_K \underline{L}_K \cdot \underline{S}_K + 4\beta_K \underline{L}_K \cdot \underline{L}_K & -4\underline{L}_K \cdot \underline{S}_K & 4\underline{L}_K \cdot \underline{L}_K \\ \hline 3\underline{L}_K \times \underline{S}_K & \underline{L}_K \times \underline{S}_K & \underline{L}_K \times \underline{S}_K \end{bmatrix}.$$

By the generalized Rayleigh quotient theorem, then for $F = \begin{bmatrix} 1 & 0 & 0 \\ 0 & 0 & 0 \\ 0 & 0 & 0 \end{bmatrix}$ and all $\underline{\iota} \in \mathbb{R}^3$

$$\underline{\iota}^T F \underline{\iota} \leq \lambda_{F,G} \underline{\iota}^T G \underline{\iota}, \quad \lambda_{F,G} = \frac{9\underline{L}_K \times \underline{S}_K}{4((3 - \alpha_K^2 + 3\beta_K^2) \underline{S}_K \cdot \underline{S}_K - 4\alpha_K \beta_K \underline{L}_K \cdot \underline{S}_K + (3 + 3\alpha_K^2 - \beta_K^2) \underline{L}_K \cdot \underline{L}_K)}.$$

In summary, we have

$$E(\zeta, v_h) \leq Ch \sum_{K \in \mathcal{T}_h} \|\zeta\|_{1,K} |v_h|_{1,K} \leq Ch \|\zeta\|_{1,\Omega} |v_h|_{1,h}.$$

The proof is completed. \square

4.3. Modulus of continuity of V_{h0}^{QRT} . Define consistency functional $E(w, \zeta_h)$ by

$$(17) \quad E(w, \zeta_h) = (w, \text{rot}_h \zeta_h) - (\text{curl } w, \zeta_h) \quad \text{for } w \in H^1(\Omega), \forall \zeta_h \in V_{h0}^{\text{QRT}}$$

$$(18) \quad E(w, \zeta_h) = (w, \text{rot}_h \zeta_h) - (\text{curl } w, \zeta_h) \quad \text{for } w \in H_0^1(\Omega), \forall \zeta_h \in V_h^{\text{QRT}}.$$

Evidently the consistency functional can be decomposed into

$$(19) \quad E(w, \zeta_h) = \sum_{K \in \mathcal{T}_h} \sum_{e \subset \partial K} \int_e (w - c_K)(\zeta_h \cdot \zeta_e - P_e(\zeta_h \cdot \zeta_e)) \, ds.$$

Here c_K is an arbitrary constant.

Theorem 19. For $w \in H^1(\Omega)$, $\zeta_h \in V_{h0}^{\text{QRT}}$ or $w \in H_0^1(\Omega)$, $\zeta_h \in V_h^{\text{QRT}}$, it holds

$$(20) \quad E(w, \zeta_h) \leq Ch |w|_{1,\Omega} \|\zeta_h\|_{\text{rot},h}.$$

Proof. Evidently, we have $\inf_{c_K \in \mathbb{R}} \|w - c_K\|_{0,\partial K}^2 \leq Ch_K |w|_{1,K}^2$. Let $\zeta_h = \gamma_1 \nabla \xi + \gamma_2 \nabla \eta + \gamma_3 \hat{\xi} \nabla \eta + \gamma_4 \hat{\eta} \nabla \xi$ and $\|\zeta_h\|_{\text{rot},K}^2 = \gamma^T V \gamma$, with $\gamma = (\gamma_1, \gamma_2, \gamma_3, \gamma_4)^T$ and

$$(21) \quad V = \begin{bmatrix} 4\zeta_K \cdot \zeta_K & -4\zeta_K \cdot \zeta_K & 0 & 0 \\ \zeta_K \times \zeta_K & \zeta_K \times \zeta_K & 0 & 0 \\ -4\zeta_K \cdot \zeta_K & 4\zeta_K \cdot \zeta_K & 0 & 0 \\ \zeta_K \times \zeta_K & \zeta_K \times \zeta_K & 0 & 0 \\ 0 & 0 & \frac{4(3+3\alpha_K^2-\beta_K^2)\zeta_K \cdot \zeta_K + 36}{9\zeta_K \times \zeta_K} & \frac{-8\alpha_K\beta_K\zeta_K \cdot \zeta_K - 36}{9\zeta_K \times \zeta_K} \\ 0 & 0 & \frac{-8\alpha_K\beta_K\zeta_K \cdot \zeta_K - 36}{9\zeta_K \times \zeta_K} & \frac{4(3+3\beta_K^2-\alpha_K^2)\zeta_K \cdot \zeta_K + 36}{9\zeta_K \times \zeta_K} \end{bmatrix}.$$

On the other hand

$$\|\zeta_h \cdot \zeta_e - P_e(\zeta_h \cdot \zeta_e)\|_{0,e}^2 = \int_e (\zeta_h \cdot \zeta_e - P_e(\zeta_h \cdot \zeta_e))^2 \, ds = \int_e \zeta_h \cdot \zeta_e (\zeta_h \cdot \zeta_e - P_e(\zeta_h \cdot \zeta_e)) \, ds,$$

then by simple calculation

$$\begin{aligned}
& \int_{e_1} \mathcal{T}_h \cdot \underline{t}_1 (\mathcal{T}_h \cdot \underline{t}_1 - P_{e_1}(\mathcal{T}_h \cdot \underline{t}_1)) \, ds \\
&= \int_{e_1} (\gamma_3 \nabla \eta \cdot \underline{t}_1 \xi + \gamma_4 \nabla \xi \cdot \underline{t}_1 \eta) \cdot (\gamma_3 \nabla \eta \cdot \underline{t}_1 (\xi - P_{e_1}(\xi)) + \gamma_4 \nabla \xi \cdot \underline{t}_1 (\eta - P_{e_1}(\eta))) \, ds \\
&= \int_{e_1} (\gamma_3 \nabla \eta \cdot \underline{t}_1)^2 \xi^2 + 2(\gamma_3 \nabla \eta \cdot \underline{t}_1)(\gamma_4 \nabla \xi \cdot \underline{t}_1) \xi \eta + (\gamma_4 \nabla \xi \cdot \underline{t}_1)^2 \eta(\eta - 1) \, ds = \frac{4(1 + \alpha_K)^2 \beta_K^2}{3|e_1|} \underline{\gamma}^T U \underline{\gamma}.
\end{aligned}$$

Here $U = \begin{bmatrix} 0 & 0 & 0 & 0 \\ 0 & 0 & 0 & 0 \\ 0 & 0 & 1 & 1 \\ 0 & 0 & 1 & 1 \end{bmatrix}$. Similarly

$$\begin{aligned}
\|\mathcal{T}_h \cdot \underline{t}_2 - P_{e_2}(\mathcal{T}_h \cdot \underline{t}_2)\|_{0,e_2}^2 &= \frac{4\alpha_K^2(-1 + \beta_K)^2}{3|e_2|} \underline{\gamma}^T U \underline{\gamma} \\
\|\mathcal{T}_h \cdot \underline{t}_3 - P_{e_3}(\mathcal{T}_h \cdot \underline{t}_3)\|_{0,e_3}^2 &= \frac{4(-1 + \alpha_K)^2 \beta_K^2}{3|e_3|} \underline{\gamma}^T U \underline{\gamma} \\
\|\mathcal{T}_h \cdot \underline{t}_4 - P_{e_4}(\mathcal{T}_h \cdot \underline{t}_4)\|_{0,e_4}^2 &= \frac{4\alpha_K^2(1 + \beta_K)^2}{3|e_4|} \underline{\gamma}^T U \underline{\gamma}.
\end{aligned}$$

By the generalized Rayleigh quotient theorem, then for all $\underline{\gamma} \in \mathbb{R}^4$

$$\|\mathcal{T}_h \cdot \underline{t}_e - P_e(\mathcal{T}_h \cdot \underline{t}_e)\|_{0,\partial K}^2 \leq C \lambda_{U,V} h_K \|\mathcal{T}_h\|_{\text{rot},K}^2.$$

Here $\lambda_{U,V} = p(\alpha_K, \beta_K, \underline{r}_K, \underline{s}_K) / q(\alpha_K, \beta_K, \underline{r}_K, \underline{s}_K)$ with

$$p(\alpha_K, \beta_K, \underline{r}_K, \underline{s}_K) = 9((3 + 3\alpha_K^2 - \beta_K^2) \underline{r}_K \cdot \underline{r}_K + 4\alpha_K \beta_K \underline{r}_K \cdot \underline{s}_K + (3 + 3\beta_K^2 - \alpha_K^2) \underline{s}_K \cdot \underline{s}_K + 36) \underline{r}_K \times \underline{s}_K$$

and

$$\begin{aligned}
q(\alpha_K, \beta_K, \underline{r}_K, \underline{s}_K) &= 4((3 + 3\alpha_K^2 - \beta_K^2)(3 + 3\beta_K^2 - \alpha_K^2)(\underline{r}_K \cdot \underline{r}_K)(\underline{s}_K \cdot \underline{s}_K) - 4\alpha_K^2 \beta_K^2 (\underline{r}_K \cdot \underline{s}_K)^2 \\
&\quad + (27 - 9\alpha_K^2 + 27\beta_K^2) \underline{s}_K \cdot \underline{s}_K - 36\alpha_K \beta_K \underline{r}_K \cdot \underline{s}_K + (27 + 27\alpha_K^2 - 9\beta_K^2) \underline{r}_K \cdot \underline{r}_K).
\end{aligned}$$

(20) follows from the Cauchy-Schwarz inequality, the proof is completed. \square

5. FINITE ELEMENT SCHEMES FOR RESPECTIVE MODEL PROBLEMS

5.1. A finite element scheme for the Poisson equation. We consider the Poisson problem with homogeneous boundary condition

$$\begin{cases} -\Delta u = f & \text{in } \Omega \\ u = 0 & \text{on } \Gamma \end{cases}$$

The variational formulation is to find $u \in H_0^1(\Omega)$, such that

$$(22) \quad \int_{\Omega} \nabla u \nabla v \, dx = \int_{\Omega} f v \, dx, \quad \forall v \in H_0^1(\Omega).$$

The finite element problem is to find $u_h \in V_{h0}^{\text{QBL}}$, such that

$$(23) \quad \sum_{K \in \mathcal{J}_h} \int_K \nabla u_h \nabla v_h \, dx = \int_{\Omega} f v_h \, dx, \quad \forall v_h \in V_{h0}^{\text{QBL}}.$$

Theorem 20. *Let $u \in H^2(\Omega) \cap H_0^1(\Omega)$ and u_h be the solutions of (22), and (23), respectively.*

Then

$$(24) \quad |u - u_h|_{1,h} \leq Ch \|u\|_{2,\Omega}.$$

Proof. The theorem is proved by the standard technique. \square

5.1.1. Numerical verification. We choose the computational domain to be the quadrilateral with vertexes $(0, 0)$, $(1, 0)$, $(2, 2)$, $(-1, 1)$. The data f is chosen such that the exact solution is the polynomial $u = y(x+y)(x-3y+4)(2x-y-2)$. We subdivide the domain with quadrilateral grids and triangle grids, respectively, and numerical solutions are computed on both grids. To generate quadrilateral grids, we use bisection strategy. To generate triangle grids, we firstly subdivide the domain with quadrilateral grids, then bisect all of them each to two triangles, see Figure 4. We first test the performance of the QBL element on the quadrilateral grids, then we test Courant element on the triangle grids as a comparison. The results are recorded in Table 3.

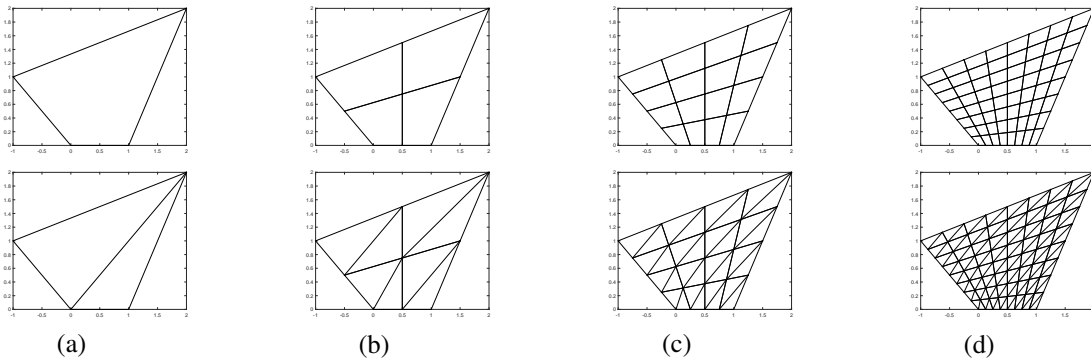


FIGURE 4. Two different sequences of grids

TABLE 3. Numerical results for Poisson problem

Size(\mathcal{T}_h)	On quadrilateral grids		On triangle grids	
	$ u - u_h _{1,h}$	$\ u - u_h\ _{0,\Omega}$	$ u - u_h _{1,h}$	$\ u - u_h\ _{0,\Omega}$
8×8	1.67E0	1.39E-1	3.59E0	2.57E-1
16×16	8.35E-1	3.52E-2	1.83E0	6.73E-2
32×32	4.18E-1	9.69E-3	9.23E-1	1.70E-2
64×64	2.09E-1	2.42E-3	4.62E-1	4.57E-3
Convergence order	1	2	1	2

Figure 5 reports on approximation results of QBL and Courant elements for Poisson equation. The x -axis and the y -axis represent the logarithm of grid size h and of the error, respectively. The dashed line and the solid line represent the error associated with the norm $|\cdot|_{1,h}$ and $\|\cdot\|_{0,\Omega}$, respectively. The results confirm our conclusion: a clear first-order of convergence is observed with $|\cdot|_{1,h}$.

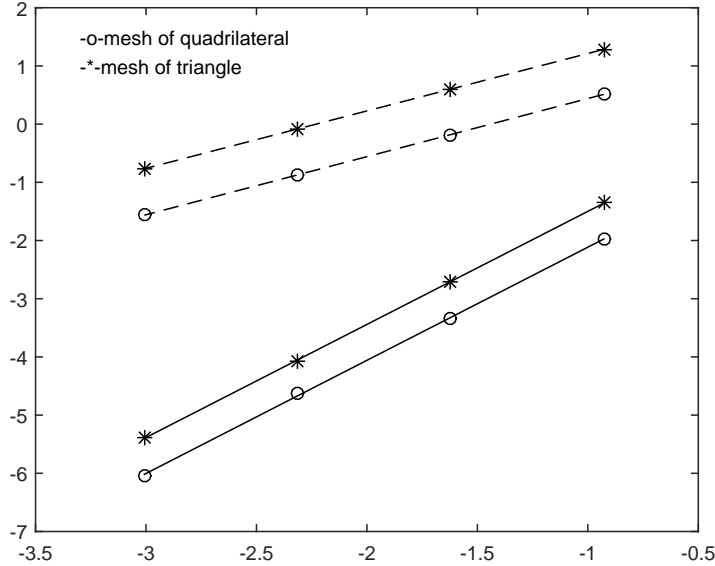


FIGURE 5. The log-log plot of the error of QBL and Courant elements for Poisson equation

5.2. Application on Laplace eigenvalue equation. We consider the Laplace eigenvalue problem with homogeneous boundary condition

$$(25) \quad \begin{cases} -\Delta u = \lambda u & \text{in } \Omega \\ u = 0 & \text{on } \Gamma. \end{cases}$$

The variational formulation is to find $(\lambda, u) \in \mathbb{R} \times H_0^1(\Omega)$, such that

$$(26) \quad \int_{\Omega} \nabla u \nabla v \, dx = \lambda \int_{\Omega} u v \, dx, \quad \forall v \in H_0^1(\Omega).$$

The finite element problem is to find $(\lambda_h, u_h) \in \mathbb{R} \times V_{h0}^{\text{QBL}}$, such that

$$(27) \quad \sum_{K \in \mathcal{J}_h} \int_K \nabla u_h \nabla v_h \, dx = \lambda_h \int_{\Omega} u_h v_h \, dx, \quad \forall v_h \in V_{h0}^{\text{QBL}}.$$

Theorem 21. *Let the eigenvalues of the problem (26) and (27) be sorted from small to big. Let (λ, u) and (λ_h, u_h) be the k -th eigenpair of (26) and (27), respectively. Then for h small enough,*

$$(28) \quad |\lambda - \lambda_h| = \mathcal{O}(h^2) \quad \text{and} \quad |u - u_h|_{1,h} = \mathcal{O}(h).$$

Proof. The theorem is proved by the standard technique. \square

5.2.1. Numerical verification. We choose the computational domain to be the unit square $\Omega = (0, 1) \times (0, 1)$. The eigenvalue λ is chosen such that the exact solution is the function $u = \sin(\pi x) \sin(\pi y)$. We first divide the computational domain into four trapezoids, then use the same strategy as Subsection 5.1 to generate the grids, see Figure 6, and repeat numerical test by same elements as before. The results are recorded in Table 4.

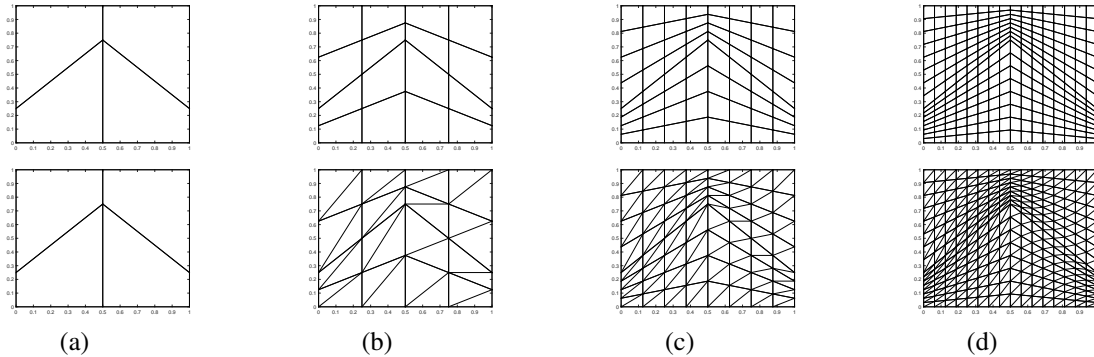


FIGURE 6. Two different sequences of grids

TABLE 4. Numerical results for Laplace eigenvalue problem

Size(\mathcal{J}_h)	On quadrilateral grids		On triangle grids		
	λ_h	$ \lambda - \lambda_h $	λ_h	$ \lambda - \lambda_h $	λ
8 × 8	2.035E1	6.090E-1	2.074E1	9.995E-1	$2\pi^2$
16 × 16	1.988E1	1.359E-1	1.998E1	2.424E-1	$2\pi^2$
32 × 32	1.977E1	3.210E-2	1.980E1	6.120E-2	$2\pi^2$
64 × 64	1.9747E1	7.800E-3	1.9754E1	1.480E-2	$2\pi^2$
Convergence order	2		2		

Figure 7 reports on approximation results of QBL and Courant elements for Laplace eigenvalue equation. The x -axis and the y -axis represent the logarithm of grid size h and of the error, respectively. In this numerical experiment, a clear second-order of convergence is observed and the numerical performance of QBL element is better than that of Courant element.

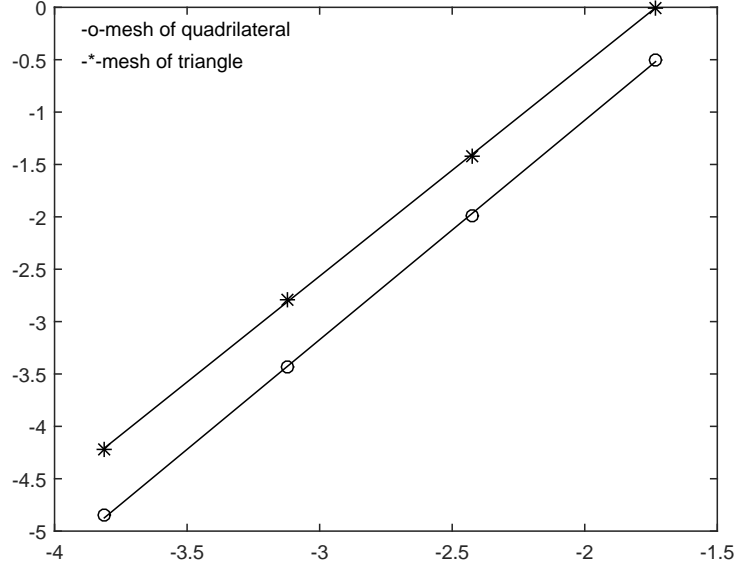


FIGURE 7. The log-log plot of the error of QBL and Courant elements for Laplace eigenvalue equation

5.3. Application on $H(\text{rot})$ equation. We consider the problem with homogeneous boundary condition

$$\begin{cases} \text{curl}(\text{rot} \underline{\sigma}) + \underline{\sigma} = \underline{f} & \text{in } \Omega \\ \underline{\sigma} \underline{t} = 0 & \text{on } \Gamma. \end{cases}$$

The variational formulation is to find $\underline{\sigma} \in H_0(\text{rot}, \Omega)$, such that

$$(29) \quad \int_{\Omega} \text{rot} \underline{\sigma} \text{rot} \underline{\tau} + \underline{\sigma} \underline{\tau} \, dx = \int_{\Omega} \underline{f} \underline{\tau} \, dx, \quad \forall \underline{\tau} \in H_0(\text{rot}, \Omega).$$

The finite element problem is to find $\underline{\sigma}_h \in V_{h0}^{\text{QRT}}$, such that

$$(30) \quad \sum_{K \in \mathcal{J}_h} \int_K \text{rot} \underline{\sigma}_h \text{rot} \underline{\tau}_h + \underline{\sigma}_h \underline{\tau}_h \, dx = \int_{\Omega} \underline{f} \underline{\tau}_h \, dx, \quad \forall \underline{\tau}_h \in V_{h0}^{\text{QRT}}.$$

Theorem 22. Let $\underline{\sigma} \in H^1(\text{rot}, \Omega) \cap H_0(\text{rot}, \Omega)$ and $\underline{\sigma}_h$ be the solutions of (29), and (30), respectively. Then

$$(31) \quad \|\underline{\sigma} - \underline{\sigma}_h\|_{\text{rot}, h} \leq Ch(|\underline{\sigma}|_{1,\Omega} + |\text{rot} \underline{\sigma}|_{1,\Omega}).$$

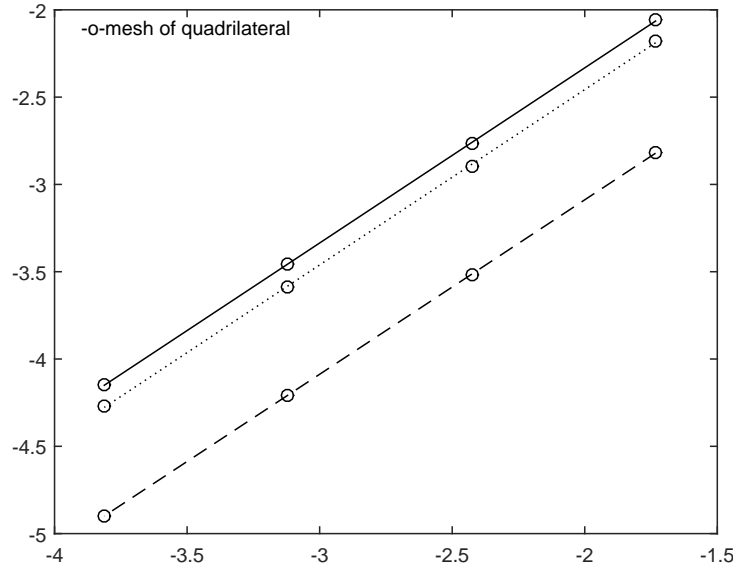
Proof. The theorem is proved by the standard technique. \square

5.3.1. *Numerical verification.* We choose the computational domain to be the unit square $\Omega = (0, 1) \times (0, 1)$. The source term f is chosen such that the exact solution is given by $\sigma = (xy^2 - xy, x^2y - xy)^T$. Then we test the performance of the QRT element on the quadrilateral grids as Subsection 5.2 and the results are recorded in Table 5.

TABLE 5. Numerical results for $H(\text{rot})$ problem

Size(\mathcal{T}_h)	$\ \sigma - \sigma_h\ _{0,\Omega}$	$ \sigma - \sigma_h _{\text{rot},h}$	$\ \sigma - \sigma_h\ _{\text{rot},h}$
8×8	1.13E-1	5.95E-2	1.28E-1
16×16	5.53E-2	2.98E-2	6.28E-2
32×32	2.78E-2	1.49E-2	3.15E-2
64×64	1.40E-2	7.45E-3	1.58E-2
Convergence order	1	1	1

Figure 8 reports on approximation results of QRT element for $H(\text{rot})$ equation. The x -axis and the y -axis represent the logarithm of grid size h and of the error, respectively. The error associated with $\|\cdot\|_{0,\Omega}$, $|\cdot|_{\text{rot},h}$ and $\|\cdot\|_{\text{rot},h}$ are plotted by dotted line, dashed line and solid line, respectively. The results confirm our conclusion: a clear first-order of convergence is observed.

FIGURE 8. The log-log plot of the error of QRT for $H(\text{rot})$ equation

6. CONCLUDING REMARKS

In this paper, we present a polynomial de Rham complex on a grid that consists of arbitrary quadrilaterals by constructing two nonconforming finite elements for the H^1 and $H(\text{rot})$ problems, respectively. As is proved in the present paper, cf. Theorem 2 and Remark 4, we can not

theoretically expect the finite element be conforming anyway; however, the two spaces are both quasi-conforming and are consistent to the requirement of the differential complex. Moreover, with respect to the $O(h^2)$ asymptotic parallelogram assumption, the scheme for $H(\text{rot})$ problem is $O(h)$ convergent for $H^1(\text{rot})$ exact solution; namely, this element does not suffer from the extra requirement on the regularity for general nonconforming $H(\text{curl})$ element (cf. [12]). For the Poisson equation, numerical experiments show that the QBL element plays superior to the triangular linear element with the same amount of unknowns for both source and eigenvalue problems, which confirms the need of quadrilateral elements.

It follows immediately that a piecewise polynomial complex can be constructed by rotation according to

$$(32) \quad \mathbb{R} \xrightarrow{\text{inclusion}} H^1 \xrightarrow{\text{curl}} H(\text{div}) \xrightarrow{\text{div}} L^2 \xrightarrow{\text{integration}} \mathbb{R}$$

by simply a rotation. Further, the methodology which use the same shape functions as that on a framework parallelogram and the nodal parameters on a physical cells can be generalized to more complicated cases, such as higher order schemes and higher dimension problems. These would be discussed in future.

REFERENCES

- [1] Todd Arbogast and Maicon R Correa. Two families of $h(\text{div})$ mixed finite elements on quadrilaterals of minimal dimension. *SIAM Journal on Numerical Analysis*, 54(6):3332–3356, 2016.
- [2] Douglas Arnold, Daniele Boffi, and Richard Falk. Approximation by quadrilateral finite elements. *Mathematics of computation*, 71(239):909–922, 2002.
- [3] Douglas N Arnold, Daniele Boffi, and Richard S Falk. Quadrilateral $h(\text{div})$ finite elements. *SIAM Journal on Numerical Analysis*, 42(6):2429–2451, 2005.
- [4] Carsten Carstensen, Joscha Gedicke, and Donsub Rim. Explicit error estimates for courant, crouzeix-raviart and raviart-thomas finite element methods. *Journal of Computational Mathematics*, pages 337–353, 2012.
- [5] Philippe G Ciarlet. *The finite element method for elliptic problems*, volume 40. Siam, 2002.
- [6] Eric Dubach, Robert Luce, and Jean-Marie Thomas. Pseudo-conforming polynomial finite elements on quadrilaterals. *International Journal of Computer Mathematics*, 86(10-11):1798–1816, 2009.
- [7] Richard S Falk, Paolo Gatto, and Peter Monk. Hexahedral $h(\text{div})$ and $h(\text{curl})$ finite elements. *ESAIM: Mathematical Modelling and Numerical Analysis*, 45(1):115–143, 2011.
- [8] Youngmok Jeon, Hyun Nam, Dongwoo Sheen, and Kwangshin Shim. A class of nonparametric dssy non-conforming quadrilateral elements. *ESAIM: Mathematical Modelling and Numerical Analysis*, 47(6):1783–1796, 2013.
- [9] Chunjae Park and Dongwoo Sheen. P 1-nonconforming quadrilateral finite element methods for second-order elliptic problems. *SIAM Journal on Numerical Analysis*, 41(2):624–640, 2003.
- [10] Lawrence E Payne and Hans F Weinberger. An optimal poincaré inequality for convex domains. *Archive for Rational Mechanics and Analysis*, 5(1):286–292, 1960.

- [11] Rolf Rannacher and Stefan Turek. Simple nonconforming quadrilateral stokes element. *Numerical Methods for Partial Differential Equations*, 8(2):97–111, 1992.
- [12] Dongyang Shi and Lifang Pei. Low order crouzeix–raviart type nonconforming finite element methods for the 3d time-dependent maxwells equations. *Applied Mathematics and Computation*, 211(1):1–9, 2009.
- [13] Zhong-Ci Shi. A convergence condition for the quadrilateral wilson element. *Numerische mathematik*, 44(3):349–361, 1984.
- [14] Shangyou Zhang. On the nested refinement of quadrilateral and hexahedral finite elements and the affine approximation. *Numerische Mathematik*, 98(3):559–579, 2004.
- [15] Shuo Zhang. Stable finite element pair for stokes problem and discrete stokes complex on quadrilateral grids. *Numerische Mathematik*, 133(2):371–408, 2016.
- [16] Zhimin Zhang. Polynomial preserving gradient recovery and a posteriori estimate for bilinear element on irregular quadrilaterals. *Int. J. Numer. Anal. Model.*, 1(1):1–24, 2004.

UNIVERSITY OF CHINESE ACADEMY OF SCIENCES, BEIJING 100190, PEOPLE'S REPUBLIC OF CHINA

E-mail address: quanqimeng@lsec.cc.ac.cn

LSEC, INSTITUTE OF COMPUTATIONAL MATHEMATICS AND SCIENTIFIC/ENGINEERING COMPUTING, ACADEMY OF MATHEMATICS AND SYSTEM SCIENCES, CHINESE ACADEMY OF SCIENCES, BEIJING 100190, PEOPLE'S REPUBLIC OF CHINA

E-mail address: jixia@lsec.cc.ac.cn

LSEC, INSTITUTE OF COMPUTATIONAL MATHEMATICS AND SCIENTIFIC/ENGINEERING COMPUTING, ACADEMY OF MATHEMATICS AND SYSTEM SCIENCES, CHINESE ACADEMY OF SCIENCES, BEIJING 100190, PEOPLE'S REPUBLIC OF CHINA

E-mail address: szhang@lsec.cc.ac.cn